Long non-coding RNA HCG18 promotes malignant phenotypes of breast cancer (BC) cells by HCG18/miR-103a-3p/UBE2O/mTORC1/HIF-1α positive feedback loop

Xu Liu
Harbin Medical University Third Hospital: Tumor Hospital of Harbin Medical University
Kun Qiao
Harbin Medical University Third Hospital: Tumor Hospital of Harbin Medical University
Kaiyuan Zhu
Harbin Medical University Third Hospital: Tumor Hospital of Harbin Medical University
Xianglan Li
Harbin Medical University Third Hospital: Tumor Hospital of Harbin Medical University
Chunbo Zhao
Harbin Medical University Third Hospital: Tumor Hospital of Harbin Medical University
Jiaqi Li
Harbin Medical University Third Hospital: Tumor Hospital of Harbin Medical University
Dawei Feng
Harbin Medical University Third Hospital: Tumor Hospital of Harbin Medical University
Yu Fang
Harbin Medical University Third Hospital: Tumor Hospital of Harbin Medical University
Peng Wang
Harbin Medical University Third Hospital: Tumor Hospital of Harbin Medical University
Cheng Qian
Harbin Medical University Third Hospital: Tumor Hospital of Harbin Medical University
Wenbo Qiao (profqiaowb@163.com)
Harbin Medical University Third Clinical College: Tumor Hospital of Harbin Medical University

---

Research

Keywords: HCG18, UBE2O, miR-103a-3p, breast cancer

Posted Date: February 26th, 2021

DOI: https://doi.org/10.21203/rs.3.rs-241505/v1

Abstract

Background: In recent years, a growing number of studies have reported that long non-coding RNAs (LncRNAs) play crucial roles in breast cancer (BC) progression and metastasis. Another study group of our research center reported that LncRNA HCG18 was one of the 30 upregulated lncRNAs in BC tissues related to normal tissues in TCGA database. However, the exactly biological roles of HCG18 in BC remains unclear.

Method: qRT-PCR was used to detect the expression profile of HCG18 in BC tissues and cell lines. In vitro assays were used to evaluate the pro-tumor function of HCG18 in BC cells. Animal study were used to explore the role of HCG18 in vivo. Bioinformatic analysis, dual-luciferase reporter assay, RNA immunoprecipitation (RIP) assay and Chromatin Immunoprecipitation (ChIP) assays were used to investigate the regulatory relationship of HCG18, miR-103a-3p, UBE2O in BC.

Results: HCG18 was upregulated in BC tissues and cells, and BC patients with high HCG18 expression tended to have poor prognosis. HCG18 could promote BC cells proliferation, invasion and provided BC cells with tumor stemness properties (CSPs) in vitro and facilitate tumor growth and lung metastasis in vivo. In terms of mechanism, HCG18 functioned as a miRNA sponge which positively regulated the expression of Ubiquitin-conjugating enzyme E2O (UBE2O) by sponging miR-103a-3p and our previous research achievement have already verified UBE2O could promote malignant phenotypes of BC cells through UBE2O/AMPKα2/mTORC1 axis. Furthermore, as a downstream target of HCG18/miR-103a-3p/UBE2O/mTORC1 axis, HIF-1α transcriptionally promoted HCG18 expression and then formed a positive feedback loop in BC.

Conclusion: HCG18 played an oncogenic role in BC and it might serve as a prognostic biomarker and a potential therapeutic target for BC treatment.

Background

Although early detection, high-quality prevention and advanced therapeutic strategies have been devoted into the clinical practice, breast cancer (BC) is still the most common female cancer diseases (30%) and the first leading cause of cancer related death (15%) worldwide[1]. Actually, the high recurrence and metastasis characteristics are the main cause of high mortality in BC. It has been reported that the overall 5-year survival rate of patients in early stage of BC is 92.5%-85.9%, however, it is decreased to 25.1% for patients in stage Ⅳ[2]. Therefore, exploring promising detection markers and developing effective therapeutic methods are urgently needed in BC.

Long non-coding RNAs (LncRNAs) are a class of RNA transcripts which are longer than 200 nucleotides in length and have no or limited protein-coding capability[3]. Recent studies have confirmed that LncRNAs are involved in a variety of physiological and pathological processes of human diseases, especially cancers[4, 5]. Another group of our research center identified LncRNA HLA complex group 18 (HCG18) was

one of the 30 upregulated LncRNAs in BC by analyzing data from two cohorts in TCGA[6]. Previously studies have also reported that HCG18 has oncogenic functions in gastric cancer, hepatocellular carcinoma, lung adenocarcinoma and colorectal cancer. However, its biological function in human BC remains unclear[7-10].

Ubiquitin-conjugating enzyme E2O (UBE2O) is a large E2-ubiquitin-conjugation enzyme which has both E2 and E3 activities[11]. Abnormal expression of UBE2O existed in many types of human cancers and deregulation of UBE2O plays crucial roles in tumor progression and metastasis[12-14]. Our previous research achievement demonstrated that UBE2O could promote BC cells proliferation, epithelial-mesenchymal transformation (EMT) and conferred BC cells with cancer stemness properties (CSPs) depending on UBE2O/AMPKα2/mTORC1-MYC positive feedback loop[15]. However, the exactly regulatory mechanism of UBE2O in BC is still needed to be further investigated.

In this study, we confirmed that HCG18 was significantly upregulated in BC patients and had closely relationship with poor prognosis in BC patients. HCG18 could promote BC cells proliferation, invasion and conferred BC cells with CSPs in vitro and facilitate tumour growth and metastasis in vivo. In terms of mechanism, we found that HCG18 could competitively adsorb miR-103a-3p, indirectly facilitating UBE2O expression and thus activating the UBE2O/mTORC1 axis in BC cells. Furthermore, as a downstream target of mTORC1, HIF-1α could transcriptionally promote HCG18 expression and constituted a positive feedback loop in BC.

Materials And Methods

BC cells and specimens

All the BC cells and normal mammary cells (MCF-10A) were purchased from the cell bank of the Chinese Academy of Sciences (Shanghai, China) and were cultured according to the supplier's instructions. Fresh BC tissues, adjacent noncancerous tissues and corresponding paraffin embedded cancer tissues (n=120) were obtained from Harbin Medical University Cancer Hospital between 2012 and 2013. All the patients rerolled in our study had complete clinicopathological information and patients who received neoadjuvant chemotherapy, radiotherapy, immunotherapy and those with recurrent tumors, bilateral BC or other previous tumors were excluded. Our study was approved by the Research Ethics Committee of Harbin Medical University and all the patients enrolled in our study had signed informed consent.

RNA extraction and quantitative real-time PCR (qRT-PCR)

Total RNA was extracted from fresh BC tissues and cells with TRIzol reagent (Invitrogen, USA) according to the manufacturer's instruction. Prime Script RT Reagent Kit with gDNA Eraser (Takara, Kyoto, Japan) was used to synthesize the cDNA and qRT-PCR was conducted using SYBR Premix Ex Taq™ II (Takara, Kyoto, Japan) on a CFX96 Touch Detection System (Bio-Rad, USA). Primers used in our study were listed

in the supplementary table S1. GAPDH , U6 and 18S tRNA were used as internal controls, and relative RNA abundances were calculated by the standard $2^{-\triangle\triangle CT}$ method.

Western blotting

Western blotting assays were performed as previously study reported[15]. Briefly, indicated cells were lysed with RIPA (Beyotime, China) buffer containing PMSF (Beyotime, China). The lysate was collected and western blotting assays were then performed. Antibodies used were listed in the supplementary table S2.

Cell proliferation assay

For the CCK-8 assays, indicated cells were seeded into 96-well plates at a density of 2×10^3 cells per well. At each pre-set time, 10μl CCK-8 reagent (Beyotime, China) were added into each well containing 90 μl culture medium and the plates were incubated at 37 °C for 2 hours. After that, the cell viability was detected by measuring the absorbance at 570 nm.

For the colony formation assays, indicated cells were seeded into six-well plates (5×10^2 cells/well) and incubated with culture medium containing 10% FBS at 37 °C for 2 weeks. After that, the cells were fixed with formalin for 30 minutes and stained with crystal violet. FluorChem M system was used to take the photos.

Edu staining assays were performed as follows: indicated cells were seeded into 96-well plates and cultured with 10% FBS medium at 37 °C. After the confluence reached to 60%-70%, the cells were subjected to Edu staining (Beyotime, China) according to the manufacture's instruction. After fixing and permeabilizing, the cells were stained with Edu and DAPI solutions. The results were captured and analyzed under a fluorescence microscope.

Scratch assays and cell invasion assays

For wound scratch assays, indicated cells were seeded into six-well plates and cultured at 37°C. After the cells reached to 95% confluence, sterile micropipette tips were used to made the scratch wounds. Then the cells were washed by PBS and cultured with medium containing 10% FBS continuously. Images were taken in schedule under a microscope at preset time and the migration rate were subsequently analyzed.

For cell invasion assays, the upper champers of 24-well transwell plates (Coring, USA) were coated with Matrigel and incubated at 37℃ for 4 hours. Then 200μl serum-free medium containing indicated cells were added into the upper champers of the transwell plates and 600 μl 10% FBS medium were added into the lower champers of the transwell plates. Then the cells were cultured at 37℃ for 24 hours. Afterwards, the non-invaded cells were scraped from the upper side of the champers and invaded cells at the under-side were fixed with 4% paraformaldehyde and stained with 1% crystal violet. Finally, the images were captured and the invaded cells were counted under a microscope.

Hematoxylin–eosin (HE) staining and immunohistochemistry (IHC)

HE staining assays were performed according to a standard HE staining technique as previously study reported[16]. Briefly, mouse lung tissues were fixed in 4% paraformaldehyde, embedded in paraffin and sectioned (5-mm thickness). After that, the lung sections were subjected to HE staining to evaluate pathological changes and photographed under an optical microscope.

IHC staining were performed on paraffin-embedded specimens from BC patients in a standard streptavidin-peroxidase complex manner. The staining results were evaluated with histochemistry score (H-score) by three senior pathologists independently. The following antibodies were used: UBE2O (Catalogue Number: 15812-1-AP, Proteintech Group, China), Ki-67 (Catalogue Number: 9449, CST, USA).

Sphere culture and sphere formation assays

For sphere formation assays, indicated cells (1×10^3) were trypsinized, resuspended with stem cell medium consisting of DMEM/F-12 (Catalogue Number: 12660012, Gibco, USA), 1×B27 (Catalogue Number: 17504044, Invitrogen, USA), 20ng/ml epidermal growth factor (Catalogue Number:PHG0311, Invitrogen, USA), 20ng/ml basic fibroblast growth factor (Catalogue Number: PHG0263, Invitrogen, USA), and 2mM L-glutamine (Catalogue Number: 25030081, Invitrogen, USA) and seeded into 24-well ultra-low attachment plates. Then the cells were cultured at 37℃ and the medium was refreshed every 48 hours. Two weeks later, the stemness spheres were observed and counted under an optical microscope.

Lentiviral production

Recombinant lentivirus for overexpression HCG18 or UBE2O in BC cells and corresponding negative controls were designed and synthesized from GenePharma (Shanghai, China). The recombinant lentivirus was transfected into indicated cells with polybrene (8μg/ml). Twenty-four hours after transfection, the cells were selected with puromycin and qRT-PCR was applied to detect the transfection efficiency.

To establish stable HCG18 or UBE2O knocking-down BC cells, shRNAs targeting HCG18 or UBE2O were designed from Sigma and transfected into indicated cells according to the manufactory's instruction. The shRNA sequences were listed in supplementary table3. qRT-PCR was used to detect the knocking-down efficiency.

Transfection of BC cells

Small interfering RNAs (siRNAs) targeting HIF-1α and its control group were designed from GenePharma. The microRNA mimics and inhibitor were synthesized by Sigma. For transfection, indicated cells were seeded into six-well plates (5×10^5 per well) and cultured at 37℃ overnight. Then the cells were transfected with corresponding victors using Lipofectamine 2000 transfection reagent (Invitrogen, USA) according to the manufacturer's instructions. Forty-eight hours later, the transfected cells were harvested for the follow-up experiments. The siRNA sequences were listed in supplementary information table3.

Subcellular fractionation

Nuclear and cytoplasmic RNA separation was conducted using PARIS™ Kit (Catalogue Number: AM1921, Invitrogen, USA) according to the manufacturer's instruction. qRT-PCR was used to analyze the expression of HCG18 in different fragments of BC cells.

RNA pull-down (RIP) assays

RIP assays were performed with Magna RIP™ RNA-Binding Protein Immunoprecipitation Kit (Millipore, USA). Briefly, indicated cells were collected and lysed with RIPA. Then the lysate was subjected to RIP with an Anti-AGO2 antibody (Abcam, USA) according to the manufacturer's instruction. Finally, the samples were disposed with proteinase K (Merck, USA) and qRT-PCR was used to analyze the binding of HCG18 and miR-103a-3p in BC cells.

Dual-luciferase reporter assay

To investigate whether miR-103a-3p could directly bind to the 3'UTR region of HCG18 or UBE2O, dual-luciferase report assays were performed using a double luciferase assay system (Promega, USA). In brief, 3'UTR region of HCG18 (wild /mutant type) or UBE2O (wild /mutant type) luciferase reporter plasmids and miR-103a-3p mimics were co-transfected into HEK-293T cells. Then the cells were lysed and luciferase assays were conducted according to the manufacturer's instruction. Firefly luciferase activity normalized to Renilla luciferase activity was used as an internal control.

To analyze whether HIF-1α could bond to the promotor region of HCG18, HCG18 promotor region (wild /mutant type) luciferase reporter plasmids and HIF-1α plasmids were co-transfected into HEK-293T cells. Forty-eight hours later, cells were harvested and dual-luciferase assays were performed. Firefly luciferase activity normalized to Renilla luciferase activity was used as an internal control.

Chromatin immunoprecipitation (ChIP)

ChIP assays were performed as previously study reported[15]. Briefly, indicated cells were treated with formaldehyde to crosslink target protein and chromatin and sonicated to an average length of 200-500bp on ice. Then a DNA depuration kit (Beyotime, China) was used to extract and clean the DNA fragments. After that, ChIP assays were conducted with an anti-HIF-1α antibody (Catalogue Number: 36169S, CST, USA) or IgG control. qRT-PCR was used to detect the promotor fragments of HCG18. The primers used in our experiment were listed in supplementary information.

Animal study

All the animal studies were approved by the Medical Experimental Animal Care Commission of Harbin Medical University and performed in Second Affiliated Hospital of the Harbin Medical University Laboratory. Animals used in our study were raised in specific pathogen-free animal facilities (Temperature was maintained at 25°C and a12 hour light–dark cycle) and provided free access to clean water and food. Animals were anesthetized with 1–3% isoflurane and humanely sacrificed by CO_2 inhalation as previous studies reported[17]. For the tumorigenesis assay, six-week-old BALB/c Nude mouse

(Vitalriver, Beijing, China) were randomly assigned into two groups (n=6), and then MDA-MB-231^{NC} or MDA-MB-231$^{HCG18\text{-}KD}$ (5×10^5) were respectively injected into the mammary fat pads of mice. The tumor growth was measured every week and seven weeks after injection, the mice were humanely sacrificed and the tumors were extracted and fixed in formalin solution. The tumor volumes were evaluated by the following formula: 1/2 (length × width^2). For the lung metastasis model, MDA-MB-231^{NC} or MDA-MB-231$^{HCG18\text{-}KD}$ (5×10^5) were respectively injected into the tail vein of the six-week-old BALB/c Nude mouse. Seven weeks after injection, the mice were humanely sacrificed and the lungs were collected to count metastatic nodules and for HE staining.

Statistical analysis

All the data were presented as the means ± SDs from at least three independent experiments. Student's t-test or one-way ANOVA test were used to analyze the differences between groups. The chi-square test was used to analyze the relationship between HCG18 expression and the clinicopathological features of the BC patients. The Kaplan–Meier method and log-rank test were applied to draw the survival curves. $P < 0.05$ indicated statistical significance, which was evaluated by GraphPad Prism 8.0 software.

Results

1. **The expression level of HCG18 was commonly upregulated in BC and was associated with poor progression of BC patients.**

Previous study reported that HCG18 was upregulated in BC tissues related to normal tissues in TCGA database[6]. However, the biological function of HCG18 in BC is largely unknown. To investigate this, we firstly detected HCG18 expression profile in BC tissues and corresponding normal breast tissues. The results showed that HCG18 was significantly upregulated in BC tissues in comparison with normal mammary tissues **(Fig.1a-b)**. **Fig.1c** exhibited that high invasive BC cells MDA-MB-231 hold the highest HCG18 expression level and the expression was relative lower in low-malignancy cells MCF-7. However, the mammary epithelial cell line MCF-10A hold the lowest HCG18 expression compared with the other BC cells. Then, we sought to assess the relevance of HCG18 expression and clinicopathologic features in BC patients. Results in **Fig.1d** and **Table 1** confirmed that HCG18 was positively correlated with the histilogical and clinical stage, tumor size and axillary lymph node metastasis of BC patients and these had been further confirmed by data from lnCAR database **(Fig.S1a-S1c)**. **Fig.1e** and **Fig.1f** showed that BC patients with high HCG18 expression had poor distant metastasis-free survival (DMFS) and overall survival (OS), and these had also been supported by survival information in Kaplan-Meier Plotter database **(Fig.1f-1h)**. Collectively, all these results revealed that HCG18 was commonly over-expressed in BC and patients with high HCG18 expression tended to have high risks of metastasis and worse progression.

2. **Aberrant expression of HCG18 was associated with proliferation, metastatic and CSPs of BC cells.**

To investigate the biological roles of HCG18 in BC cells, we employed HCG18 highly expressed cell line MDA-MB-231 and low HCG18 expressed cell line MCF-7 for further experiments. Three set of specific shRNAs targeting HCG18 were transfected into MDA-MB-231 cells to generate HCG18 knocking-down cells (MDA-MB-231$^{HCG18\text{-}KD1}$, MDA-MB-231$^{HCG18\text{-}KD2}$ and MDA-MB-231$^{HCG18\text{-}KD3}$) and HCG18 was stably over-expressed in MCF-7 cells (MCF-7^{HCG18}). The HCG18 expression profile in generated cells were detected by qRT-PCR. **Fig.S1d** showed that HCG18-KD1 and HCG18-KD2 yielded a relatively batter knocking-down efficiency in MDA-MB-231 and HCG18 was significantly over-expressed in MCF-7^{HCG18}, so MDA-MB-231$^{HCG18\text{-}KD1}$, MDA-MB-231$^{HCG18\text{-}KD2}$ and MCF-7^{HCG18} were applied in the following experiments. Next, CCK-8 assays were performed to detect the effect of HCG18 in proliferation. **Fig.2a** revealed that the proliferation capability was significantly decreased after knocking down HCG18 in MDA-MB-231 cells, and MCF-7^{HCG18} exhibited a better proliferation ability compared with the control group. Colony formation assays **(Fig.2b)** and Edu staining assays **(Fig.2c)** further confirmed this conclusion. Then, Ki-67 (Ki-67 was regarded as an important index of tumor growth in BC) expression state was detected in BC tissues by IHC and chi-square test was used to analyze the relationship between HCG18 and Ki-67 expression. **Fig.2d** revealed that there was a positive correlation between HCG18 and Ki-67 expression in clinical samples of BC patients. To verify the effect of HCG18 on tumorigenesis in vivo, MDA-MB-231^{NC} and MDA-MB-231$^{HCG18\text{-}KD1}$ were orthotopically injected into the mammary fat pads of BALB/c nude mice. As was shown in **Fig.2e**, knocking-down HCG18 significantly suppressed the tumor growth and prolonged tumor-free survival in comparison with the control group. Taken together, all these results exhibited that HCG18 could promote BC cells proliferation both in vitro and in vivo.

Results in table1 showed that there was a closely relationship between HCG18 expression and the status of axillary lymph node metastasis in BC patients, so we focused on the pro-metastasis function of HCG18 in BC cells. Wound healing assays showed that the migration ability was extremely decreased after knocking-down HCG18 in MDA-MB-231, and the migration ability of MCF-7^{HCG18} was increased in comparison with the control group **(Fig.3a)**. Matrigel invasion assays also exhibited the similar results **(Fig.3b)**. Western blotting assays revealed that the epithelial related protein E-cadherin was increased, but the mesenchymal marker vimentin and metastatic markers MMP2 and MMP9 were declined in MDA-MB-231$^{HCG18\text{-}KD}$ cells. The opposite results were observed in MCF-7^{HCG18} compared with the control group **(Fig.3d)**.

In recent years, a growing number of studies have reported that CSPs played important roles in tumor survival, proliferation, invasion, immune escape and drug resistance. Then the following experiments were sought to explore the relationship between HCG18 expression and CSPs in BC cells. Sphere formation assays revealed that the sphere formation ability of MDA-MB-231$^{HCG18\text{-}KD}$ was obviously declined compared with the control group, however the capability of CSPs was remarkably enhanced after overexpressing HCG18 in MCF-7 cells (**Fig.3c**). Western blotting assays showed that CSP markers CD44, ABCG2 and OCT4 were remarkably decreased in MDA-MB-231$^{HCG18\text{-}KD}$ and increased in MCF-7^{HCG18} compared with the control group **(Fig.3e)**. Finally, lung metastasis mouse models were employed to investigate the pro-metastasis function of HCG18 in vivo. The results showed that mice injected with

MDA-MB-231$^{HCG18\text{-}KD}$ exhibited fewer metastasis nodes compared with the mice in control group **(Fig.3e-3f)**. In conclusion, all these results confirmed that HCG18 could provide BC cells with CSPs in vitro and promoted BC cells metastasis both in vitro and in vivo.

3. **UBE2O contributed to the tumor promoting function of HCG18 in BC cells.**

E2s play important roles in regulating cellular post-translational protein modifications and are involved in a wide range of key physiological or pathologic processes. Multiple studies have reported that aberrant E2s expression is commonly existed in a variety of human cancers. Some cancer related E2s could facilitate DNA repair, cell cycle progression and activate oncogenic signaling pathways, which promote cancer progression and metastasis[18]. Our previous study reported that ubiquitin-conjugating enzyme E2O (UBE2O) could promote the proliferation, EMT and provide BC cells with CSPs by degrading AMPKα2, thus activating mTORC1-MYC axis[15]. For this reason, we hypothesized there may be a potential interaction network between HCG18 and E2s in BC. Then a panel of cancer related E2s were detected in MDA-MB-231^{NC}/MDA-MB-231$^{HCG18\text{-}KD}$ and MCF-7^{NC}/MCF-7^{HCG18} cells. Coincidentally, we found that there was a closely positive association between HCG18 and UBE2O expression in the indicated cells (**Fig.4a and Fig.S1e-f**). To further confirm this, correlation analysis was performed using GEPIA database. The results revealed that HCG18 expression was positively correlated with UBE2O expression in BC **(Fig.4b)**, and this correlation was further verified in clinical samples (**Fig.4c-d**). Next, we knocked down UBE2O in MCF-7^{HCG18} (MCF-7$^{HCG18+UBE2O\text{-}KD}$) and over-expressed UBE2O in MDA-MB-231$^{HCG18\text{-}KD1}$ cells (MDA-MB-231$^{HCG18\text{-}KD+UBE2O}$) **(Fig.4e)**. Western blotting assays revealed that the enhanced expression of E-cadherin and the declined expression of vimentin, MMP2, MMP9, CD44 and OCT4 were reversed in MDA-MB-231$^{HCG18\text{-}KD+UBE2O}$ cells, and the opposite results were observed in MCF-7$^{HCG18+UBE2O\text{-}KD}$ compared with the control group **(Fig.4f)**.

Then we explored the effect of UBE2O on the protumor function of HCG18 in BC cells in vitro. CCK-8 **(Fig.5a)**, clone formation assays **(Fig.5b)** and Edu staining assays **(Fig.5c)** showed that over-expressing UBE2O could significantly reverse the declining proliferation ability of MDA-MB-231$^{HCG18\text{-}KD}$, and the enhanced multiplication capacity was abolished after knocking-down UBE2O in MCF-7^{HCG18} cells. **Fig.5d-5e** and **Fig.6a** showed that the migration, invasion and sphere formation capabilities of MDA-MB-231$^{HCG18\text{-}KD+UBE2O}$ were improved compared with the MDA-MB-231$^{HCG18\text{-}KD}$, and knocking down UBE2O in MCF-7^{HCG18} remarkably destroyed these capabilities in comparison with the control group. Taken together, all these results above confirmed that UBE2O played a vital role in the cancer-promoting function of HCG18 in BC cells.

4. **HCG18 promoted the expression of UBE2O by sponging miR-103a-3p in BC cells**

To further identify the regulatory mechanism of UBE2O by HCG18 in BC cells, we firstly ascertained the cellular location of HCG18 in BC cells. Subcellular fraction assays exhibited that HCG18 were predominantly distributed in the cytoplasm of BC cells **(Fig.6b)**, which was further confirmed by lncLocator database **(Fig.S1g)** and in accordance with previous studies reported[19, 20]. Recently, many

studies confirmed that cytoplasmic lncRNAs could affect the biological process of BC cells by modulating the expression of miRNAs in a competing endogenous RNA (ceRNA) dependent manner[15, 21]. Therefore, we speculated that HCG18 could influence the stability of UBE2O in a ceRNA mechanism. To validated this, Targerscan, miRwalk and starbase were used to predicted the potential miRNAs, and the results in **Fig.6c** revealed that there were three miRNAs (miR-30a-5p, miR-34a-5p and miR-103a-3p) connected with both HCG18 and UBE2O. Then we knocked down HCG18 in MDA-MB-231 and MCF-7 cells and qRT-PCR was applied to detected the expression change of the three miRNAs above. The results showed that compared with the control group, the expression level of miR-103a-3p was remarkably increased after knocking-down HCG18 both in MDA-MB-231 and MCF-7 cells. However, there were no expression changes of the other two miRNAs in the indicated cells **(Fig.6d)**. We firstly explored the interaction between HCG18 and miR-103a-3p in the following experiments. Dual-luciferase assays revealed that transfection of miR-103a-3p mimics could significantly reduce the luciferase activity of HCG18-WT group but failed to affect that of the mutant one **(Fig.6e)**. Anti-AGO2 RIP assays further confirmed their binding potential **(Fig.7a)**. Then the expression level of miR-103a-3p was detected in BC tissues and corresponding normal tissues. The results exhibited that miR-103a-3p was obviously decreased in BC tissues **(Fig.7b)**, and there was a negative relationship between miR-103a-3p and HCG18 in BC tissues **(Fig.7c)**. Collectively, all these results revealed that HCG18 acted as a sponge for miR-103a-3p in BC cells.

Then we validated whether miR-103a-3p could mediate the function of HCG18 in promoting UBE2O expression. The results in **Fig.7d** showed that ectopic expression of miR-103a-3p by miRNA mimics obviously reduced UBE2O mRNA expression in the indicated cells. Dual-luciferase assays further revealed that overexpression of miR-103a-3p could decrease the luciferase activity of the wild-type UBE2O reporter but not the mutant one, which indicated that UBE2O was a directly target of miR-103a-3p **(Fig.7e)**. Correlation analysis in **Fig.7f** identified that UBE2O expression was negatively correlated with miR-103a-3p expression in BC tissues. Taken together, all these results above claimed that HCG18 promoted UBE2O expression by sponging miR-103a-3p in human BC.

5. **HIF-1α transcriptionally promoted HCG18 expression in BC cells.**

Since we verified that HCG18 was upregulated in BC, the subsequent experiments were carried out to explore the regulatory mechanism resulting in the aberrant expression of HCG18 in BC. JASPAR database was applied to identify the potential HCG18 transcription factors and coincidentally, we found that there were four potential binding sites for HIF-1α in the promotor region of HCG18 **(Fig.8a)**. Our previous study demonstrated that UBE2O could active mTORC1 signaling pathway by meditating AMPKα2 ubiquitination, and mTORC1 was associated with controlling HIF-1α expression, which in turn promoted cell growth and anabolism[15, 22, 23]. Therefore, HIF-1α was knocked down in MDA-MB-231 and MCF-7 cells. The efficiency of HIF-1α silencing were detected by qRT-PCR, as well as the relative HCG18 expression. The results in **Fig.8b** revealed that HCG18 was significantly declined after knocking down HIF-1α in the indicated cells. Correlation analysis showed that there was a positive relationship between HIF-1α and HCG18 expression in BC tissues **(Fig.8c)**, and this had been further confirmed by GEPIA database

(Fig.8d). Then four sets of luciferase reporter plasmids containing the wild-type or mutant type of HCG18 promotor region were constructed and dual-luciferase assays were performed to validate the potential HIF-1α binding sties. The results claimed that for site 2, transfecting HIF-1α plasmids could significantly increase the luciferase activity of WT group but not the mutant one. For the other three sites, however, there were no differences of luciferase activity in both WT and mutant groups after transfecting HIF-1α plasmids **(Fig.7e)**. These results indicated that HIF-1α could bind to the promotor region of HCG18 (site2) and facilitated HCG18 transcription. This conclusion had been further confirmed by ChIP assays **(Fig. 7f)**. Taken together, all these results above demonstrated that HIF-1α could promote HCG18 expression, thus forming a positive feedback in BC cells **(Fig.9)**.

Discussion

From the results above, we can draw the following conclusion: (1) HCG18 was upregulated in BC tissues and patients with high HCG18 expression tended to have a poor prognosis. (2) HCG18 could promote BC cells proliferation, invasion and CSPs in vitro and facilitate breast tumor growth and metastasis in vivo. (3) HCG18 endowed the malignant phenotype of BC cells by sponging miR-103a-3p, indirectly enhancing UBE2O expression and activating mTORC1 signaling pathway. (4). As a downstream target of mTORC1 axis, HIF-1α could transcriptionally promote HCG18 expression and constitute a positive feedback loop in BC.

HCG18 was identified as one of the 30 upregulated LncRNAs in BC by analyzing data from two cohorts in TCGA database[6]. However, its exact expression profile and biological function in BC remains undetermined. Therefore, we detected HCG18 expression in BC tissues for the first time and the results were consisted with the result in TCGA database. We found HCG18 hold a high expression profile in BC tissues and cells. Furthermore, we found that BC patients with high HCG18 expression had worse DMFS and OS, and these results were further confirmed by survival information from Kaplan-Meier Plotter database. Then we established stable $HCG18^{KD}$ /$HCG18^{OE}$ BC cells and employed both in vitro and in vivo assays to evaluate HCG18's biological function. All the results certified that HCG18 served as an oncogene by promoting proliferation, invasion and providing CSPs in BC cells. Previously studies also reported that HCG18 played tumor promotor roles in many other types of carcinomatosis. HCG18 could increase the expression level of WIPF1, DNAJB12 and activate PI3K/AKT axis in gastric cancer cells, thus promoting gastric cancer progression[7, 9, 10]. HCG18 could contribute to hepatocellular carcinoma progression by improving CENPM expression[8]. HCG18 could also act as an oncogene in lung adenocarcinoma through enhancing HMMR expression and accelerate nasopharyngeal carcinoma progression by upregulating CCND1[9, 24]. All these achievements above portended that HCG18 may be a potential diagnostic marker and a novel anti-tumor target for cancer therapy. Our research expanded our knowledge on the role of HCG18 in human malignant neoplastic diseases.

UBE2O is a large E2 ubiquitin-conjugation enzyme which acts as a combination of E2 and E3 enzymes and has both E2 and E3 activities[11]. Deregulation of UBE2O has been associated with several human

diseases, especially cancers. UBE2O could mediate Mxi1 ubiquitination and then promote lung cancer progression and radioresistance[25]. It has been reported that UBE2O could decrease the stability of MLL in a polyubiquitination-dependent manner, which results in aggressive leukaemia[26]. Our previous achievement proved that UBE2O could promote BC cells proliferation, EMT and provide BC cells with CSPs by UBE2O/AMPKα2/mTORC1/MYC positive feedback loop[15]. However, as an important oncoprotein, the regulatory mechanism of UBE2O hasn't been elaborated in detail. In this study, we found that there was a positively relationship between HCG18 and UBE2O expression in BC cells and tissues. To further investigate this, we performed bioinformatic analysis, luciferase assays and RIP assays with the Ago2 protein. All these results confirmed that UBE2O was a directly downstream target of miR-103a-3p and HCG18 could enhanced UBE2O mRNA stability by competitively absorbing miR-103a-3p and in a competing endogenous RNAs (ceRNAs) dependent manner. Furthermore, we firstly verify that miR-103a-3p was downregulated in BC tissues and serves as a tumor suppressor in BC. Chang JT. *et al* analyzed miRNA expression profile and their relationship with prognosis of BC patients in TCGA database. They reported that miR-103a-3p was decreased in BC tissues and contributed to a better prognosis of BC patients [27]. Our result was in accordance with previous study and further expanded our knowledge about regulatory mechanism of UBE2O in BC.

HIF-1α is a crucial regulator of metabolism and a well characterized oncoprotein in cancer cells[28]. Through modulating a series of glycolytic enzyme gene expression, HIF-1α could stimulate angiogenesis, enhance aerobic glycolysis and mediate metabolic reprogramming, which in turn facilitates BC cells malignant transformation[29]. HIF-1α could also bind to the hypoxia response regions (HREs) in the promotor region of target genes and acts as a transcriptional factor in regulating multiple cancer-related genes expression[30]. Several LncRNAs participating in tumorigenesis and metastasis have been proved to be regulated by HIF-1α mediated transcriptional regulation, such as LncRNA EFNA3, LncRNA BCRT1 and LncRNA HITT[15, 31, 32]. In our study, we identified HIF-1α maybe a potential transcriptional factor of HCG18 and we found there were four potential HREs in the promoter region of HCG18 by JASPAR database. Knocking down HIF-1α could suppress HCG18 expression in BC cells and there was a positive correlation between HCG18 and HIF-1α expression in both BC tissues and GEPIA database. ChIP and dual-luciferase reporter assay further confirmed that HIF-1α could bind to the specific HREs in the promoter region of HCG18 and promote HCG18 expression in BC cells. This self-control positive feedback loop further highlights the significance of the HCG18/miR-103a-3p/UBE2O/mTORC1-HIF-1α axis in BC.

Conclusion

Our study confirmed that HCG18 functioned as a miRNA sponge to positively regulate UBE2O expression through sponging miR-103a-3p and subsequently mediated the malignant phenotypes of BC cells, thus playing an oncogenic role in BC progression. Our research provided a new theoretical basis for exploring the mechanism of the proliferation, invasion and CSPs in BC cancer. Collectively, our study firstly demonstrated that HCG18/miR-103a-3p/UBE2O/mTORC1-HIF-1α axis constituted a positive feedback

loop in promoting proliferation, invasion and providing CSPs in BC. HCG18 could become a promising therapeutic target and prognostic predictor against BC.

Abbreviations

BC: breast cancer; CCK-8: cell counting kits-8; ChIP: Chromatin immunoprecipitation; CSPs: cancer stemness properties; DMFS: distant metastasis-free survival; EMT: epithelial-mesenchymal transformation; HCG18: HE: Hematoxylin–eosin; HLA complex group 18; IHC: immunohistochemistry; LncRAN: long non-coding RNA; OS: overall survival; qRT-PCR: quantitative real-time PCR; siRNAs: Small interfering RNAs; UBE2O: Ubiquitin-conjugating enzyme E2O; RIP: RNA pull-down.

Declarations

Ethics approval and consent to participate

This study was conducted in accordance with the Declaration of Helsinki principles. It was approved by the Research Ethics Committee of Harbin Medical University.

Consent for publication

All materials and images are original. No consent needs to declare.

Availability of data and material

The data in the present study are available from the corresponding authors upon reasonable request.

Competing interests

The authors declare that they have no competing interests.

Funding

This work was supported by China Postdoctoral Science Foundation (Grant Number: 2020M681116) and Heilongjiang Province Postdoctoral Science Foundation (Grant Number: LBH-Z20181).

Authors' contributions

XL: Conception, design, collection and assembly of data, participate in all experiments, manuscript writing; KQ: Conception, design, manuscript writing; KyZ: In vitro experiments, manuscript writing; XlL: Collection and assembly of data; CbZ: Animal study, manuscript writing; JqL: Collection and assembly of data; DwF: Cases collection and IHC staining and scoring, manuscript writing; PW: Cases collection and IHC staining and scoring; YF: Collection and assembly of data; ZpX: Manuscript writing; CQ: Funding, conception and design, manuscript writing; WbQ: Funding, conception and design, manuscript writing.

Acknowledgements

We sincerely appreciate researchers who worked for this experiment

References

1. Siegel R L, K D Miller, H E Fuchs & A Jemal Cancer Statistics, 2021. CA Cancer J Clin 2021,71,7-33.
2. Wang F, X Shu, I Meszoely, T Pal, I A Mayer, Z Yu et al. Overall Mortality After Diagnosis of Breast Cancer in Men vs Women. JAMA Oncol 2019.
3. Wilusz J E, H Sunwoo & D L Spector Long noncoding RNAs: functional surprises from the RNA world. Genes Dev 2009,23,1494-1504.
4. Cabili M N, C Trapnell, L Goff, M Koziol, B Tazon-Vega, A Regev et al. Integrative annotation of human large intergenic noncoding RNAs reveals global properties and specific subclasses. Genes Dev 2011,25,1915-1927.
5. Geisler S & J Coller RNA in unexpected places: long non-coding RNA functions in diverse cellular contexts. Nat Rev Mol Cell Biol 2013,14,699-712.
6. Xu S, D Kong, Q Chen, Y Ping & D Pang Oncogenic long noncoding RNA landscape in breast cancer. Mol Cancer 2017,16,129.
7. Liu Y, W Lin, Y Dong, X Li, Z Lin, J Jia et al. Long noncoding RNA HCG18 up-regulates the expression of WIPF1 and YAP/TAZ by inhibiting miR-141-3p in gastric cancer. Cancer Med 2020.
8. Zou Y, Z Sun & S Sun LncRNA HCG18 contributes to the progression of hepatocellular carcinoma via miR-214-3p/CENPM axis. J Biochem 2020,168,535-546.
9. Ma F, K An & Y Li Silencing of Long Non-Coding RNA-HCG18 Inhibits the Tumorigenesis of Gastric Cancer Through Blocking PI3K/Akt Pathway. Onco Targets Ther 2020,13,2225-2234.
10. Ma P, L Li, F Liu & Q Zhao HNF1A-Induced lncRNA HCG18 Facilitates Gastric Cancer Progression by Upregulating DNAJB12 via miR-152-3p. Onco Targets Ther 2020,13,7641-7652.
11. Berleth E S & C M Pickart Mechanism of ubiquitin conjugating enzyme E2-230K: catalysis involving a thiol relay? Biochemistry 1996,35,1664-1671.
12. Toffoli S, I Bar, F Abdel-Sater, P Delree, P Hilbert, F Cavallin et al. Identification by array comparative genomic hybridization of a new amplicon on chromosome 17q highly recurrent in BRCA1 mutated triple negative breast cancer. Breast Cancer Res 2014,16,466.
13. Rice K L, X Lin, K Wolniak, B L Ebert, W Berkofsky-Fessler, M Buzzai et al. Analysis of genomic aberrations and gene expression profiling identifies novel lesions and pathways in myeloproliferative neoplasms. Blood Cancer J 2011,1,e40.
14. Lin M, L T Smith, D J Smiraglia, R Kazhiyur-Mannar, J C Lang, D E Schuller et al. DNA copy number gains in head and neck squamous cell carcinoma. Oncogene 2006,25,1424-1433.
15. Liang Y, X Song, Y Li, B Chen, W Zhao, L Wang et al. LncRNA BCRT1 promotes breast cancer progression by targeting miR-1303/PTBP3 axis. Mol Cancer 2020,19,85.

16. Chong B F, J E Murphy, T S Kupper & R C Fuhlbrigge E-selectin, thymus- and activation-regulated chemokine/CCL17, and intercellular adhesion molecule-1 are constitutively coexpressed in dermal microvessels: a foundation for a cutaneous immunosurveillance system. J Immunol 2004,172,1575-1581.
17. Liu H, Y Liu, P Sun, K Leng, Y Xu, L Mei et al. Colorectal cancer-derived exosomal miR-106b-3p promotes metastasis by down-regulating DLC-1 expression. Clin Sci (Lond) 2020,134,419-434.
18. Voutsadakis I A Ubiquitin- and ubiquitin-like proteins-conjugating enzymes (E2s) in breast cancer. Mol Biol Rep 2013,40,2019-2034.
19. Li W, T Pan, W Jiang & H Zhao HCG18/miR-34a-5p/HMMR axis accelerates the progression of lung adenocarcinoma. Biomed Pharmacother 2020,129,110217.
20. Xu Z, B Huang, Q Zhang, X He, H Wei & D Zhang NOTCH1 regulates the proliferation and migration of bladder cancer cells by cooperating with long non-coding RNA HCG18 and microRNA-34c-5p. J Cell Biochem 2019,120,6596-6604.
21. Ni C, Q Q Fang, W Z Chen, J X Jiang, Z Jiang, J Ye et al. Breast cancer-derived exosomes transmit lncRNA SNHG16 to induce CD73+gammadelta1 Treg cells. Signal Transduct Target Ther 2020,5,41.
22. Vila I K, Y Yao, G Kim, W Xia, H Kim, S J Kim et al. A UBE2O-AMPKalpha2 Axis that Promotes Tumor Initiation and Progression Offers Opportunities for Therapy. Cancer Cell 2017,31,208-224.
23. Laplante M & D M Sabatini mTOR signaling in growth control and disease. Cell 2012,149,274-293.
24. Li L, T T Ma, Y H Ma & Y F Jiang LncRNA HCG18 contributes to nasopharyngeal carcinoma development by modulating miR-140/CCND1 and Hedgehog signaling pathway. Eur Rev Med Pharmacol Sci 2019,23,10387-10399.
25. Huang Y, X Yang, Y Lu, Y Zhao, R Meng, S Zhang et al. UBE2O targets Mxi1 for ubiquitination and degradation to promote lung cancer progression and radioresistance. Cell Death Differ 2020.
26. Liang K, A G Volk, J S Haug, S A Marshall, A R Woodfin, E T Bartom et al. Therapeutic Targeting of MLL Degradation Pathways in MLL-Rearranged Leukemia. Cell 2017,168,59-72 e13.
27. Chang J T, F Wang, W Chapin & R S Huang Identification of MicroRNAs as Breast Cancer Prognosis Markers through the Cancer Genome Atlas. PLoS One 2016,11,e0168284.
28. Gilkes D M & G L Semenza Role of hypoxia-inducible factors in breast cancer metastasis. Future Oncol 2013,9,1623-1636.
29. Wilson W R & M P Hay Targeting hypoxia in cancer therapy. Nat Rev Cancer 2011,11,393-410.
30. Lee P, N S Chandel & M C Simon Cellular adaptation to hypoxia through hypoxia inducible factors and beyond. Nat Rev Mol Cell Biol 2020,21,268-283.
31. Wang X, L Li, K Zhao, Q Lin, H Li, X Xue et al. A novel LncRNA HITT forms a regulatory loop with HIF-1alpha to modulate angiogenesis and tumor growth. Cell Death Differ 2020,27,1431-1446.
32. Gomez-Maldonado L, M Tiana, O Roche, A Prado-Cabrero, L Jensen, A Fernandez-Barral et al. EFNA3 long noncoding RNAs induced by hypoxia promote metastatic dissemination. Oncogene 2015,34,2609-2620.

Table

Table1 Association HCG18 expression and patients'clinicopathological characteristics in invasive ductal carcinoma tissues				
characteristics	**HCG18 expression**		**No.**	**P-value**
	high	low		
Age			120	ns
≤ 40	5	5		
> 40	49	61		
ER/PR			120	
(+)	24	38		ns
(-)	30	28		
HER-2			120	ns
0-2 (+)	36	30		
3 (+)	18	21		
ki67			120	**0.0431***
≤ 20%	22	40		
> 20%	32	26		
Tumor size			120	**0.0259***
T1	17	35		
T2-T3	37	31		
Axillary lymph node metastasis			120	**0.0002*****
N0	22	50		
N1-N3	32	16		
Histological grade				
1-2 grade	38	54	120	Ns
3 grade	16	12		
clinical stages			120	**<0.0001**
I-II A	19	55		
II B-III	35	11		
Statistically significant difference (P < 0.05) was indicated in bold letters				

Figures

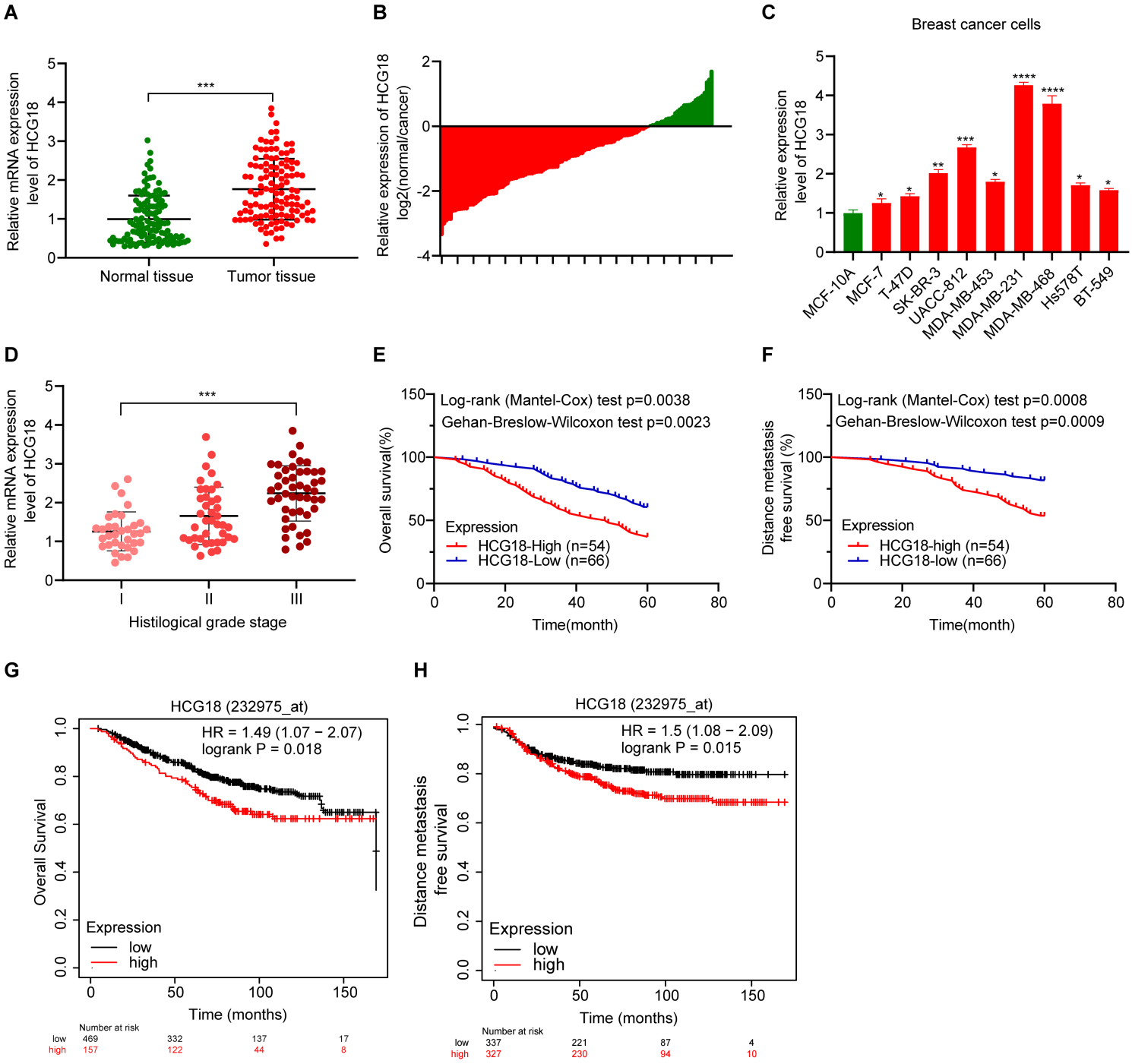

Figure 1

a-b qRT-PCR was used to detect the expression profile of HCG18 in BC tissues and compared normal mammary tissues (n=120). c HCG18 was examined in a panel of BC cell lines and normal breast epithelial cell line by qRT-PCR. d qRT-PCR was applied to measure the HCG18 expression in different clinical stages of BC patients. e-f Kaplan–Meier analysis showed that BC patients with high HCG18 expression had worse DMFS or OS then those with low HCG18 expression (n=120). g-h Survival

information of BC patients with high or low HCG18 expression were obtained from KM-plot database. *p < 0.05, **p < 0.01, ***p < 0.001. The data represent at least three independent experiments.

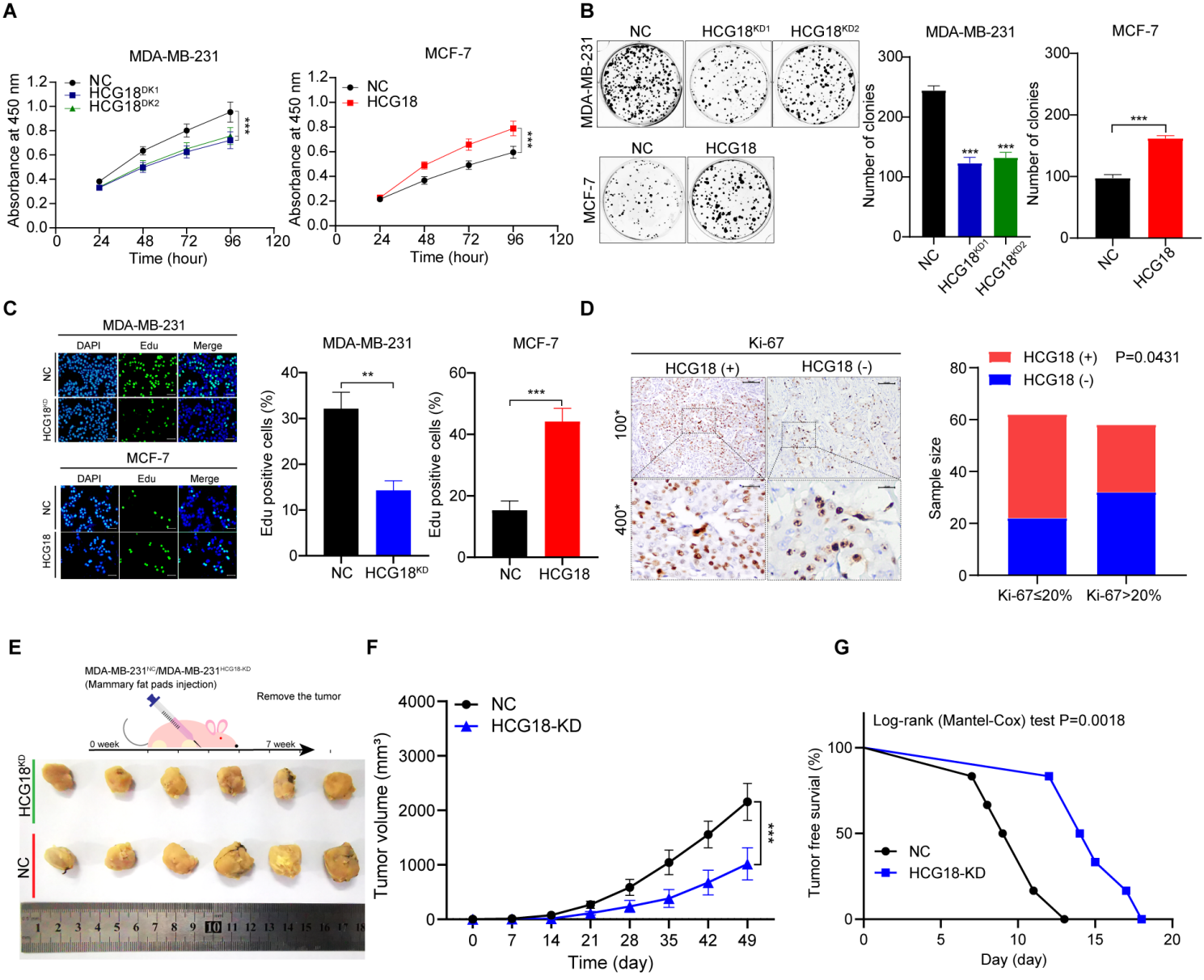

Figure 2

a-b CCK-8 and colony formation assays were performed to detect the proliferation ability of MDA-MB-231NC/MDA-MB-231HCG18-KD and MCF-7NC/MCF-7HCG18 cells. c Edu staining assays showed that HCG18 promoted BC cells proliferation in vitro. d The expression level of Ki-67 in BC patients was detected by IHC (upper: magnification × 100, Scale bar, 100 μm; lower: magnification × 400, Scale bar, 20 μm), and the correlation between HCG18 and Ki-67 was analyzed by a chi-square test (Ki-67<20 % was regarded as low expression). e-g Mouse xenograft models were employed to investigate the tumorigenesis of MDA-MB-231NC/MDA-MB-231HCG18-KD in vivo (e), the volumes of tumors were recorded (f) and the tumor free survival of the two groups were analyzed (g). The data are shown as the mean ± s.d. Student's t test was used for statistical analysis: *p < 0.05, **p < 0.01, ***p < 0.001. The data represent at least three independent experiments.

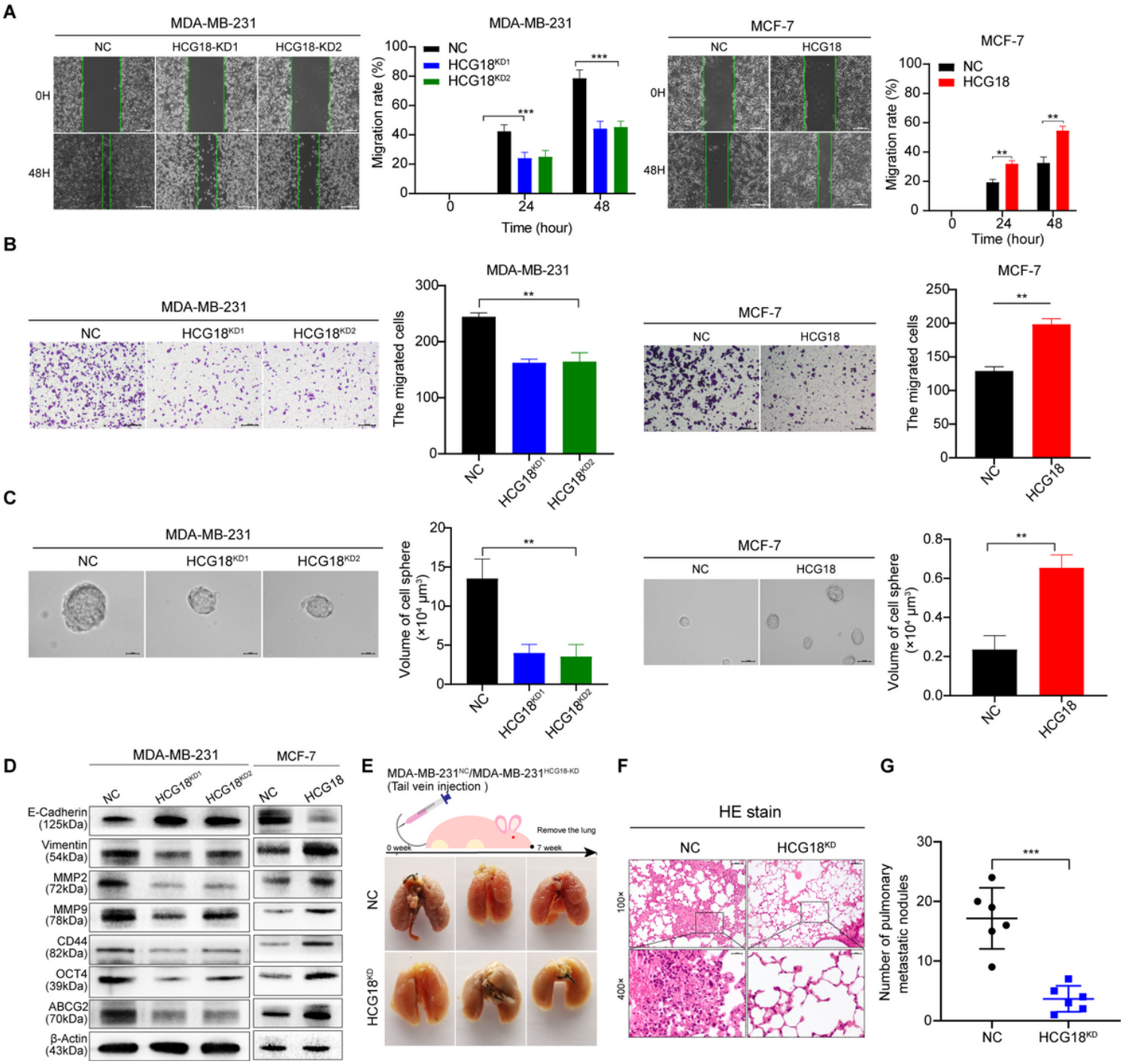

Figure 3

a Wound healing assays were performed to detected the effect of HCG18 on migration ability in the indicated cells. b Invasion capability of MDA-MB-231NC/MDA-MB-231HCG18-KD and MCF-7 NC/MCF-7HCG18cells were examined by Matrigel invasion assays. c Spheroid-formation capabilities of BC cells after changing HCG18 expression were examined by tumor sphere formation assays. d The expression level of EMT markers (E-cadherin and vimentin), metastatic markers (MMP-2 and MMP-9) and CSPs markers (CD44, OCT4 and ABCG2) were determined by western blotting assays. e-g Lungs excised from MDA-MB-231NC/MDA-MB-231HCG18-KD mice were photographed (e), and subjected to HE staining (f), and then the nodes of lung metastasis were analyzed (g). The data are shown as the mean ± s.d.

Student's t test was used for statistical analysis: *p < 0.05, **p < 0.01, ***p < 0.001. The data represent at least three independent experiments.

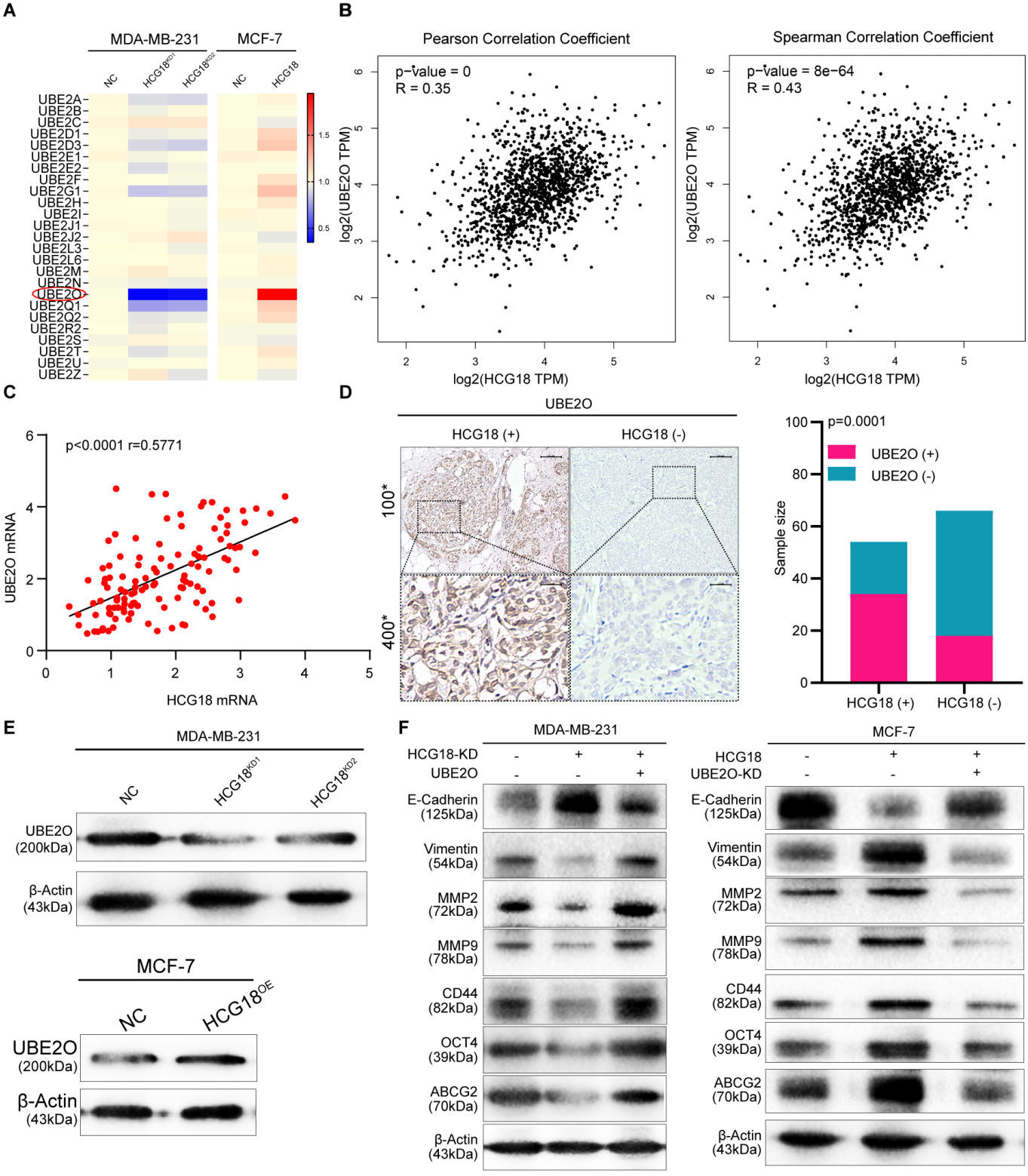

Figure 4

a The expression level of predicted tumor related E2s targeted HCG18 were analyzed in MDA-MB-231NC/MDA-MB-231HCG18-KD and MCF-7NC/MCF-7HCG18 cells. b Results from GEPIA database indicated that UBE2O expression was negatively correlated with HCG18 expression in BC. c The

expression level of UBE2O in BC patients was detected by qRT-PCR and correlation analysis was used to detect the relationship between UBE2O and HCG18 in BC patients. d The protein expression level of UBE2O was detected by IHC in BC tissues (The staining results were evaluated with a standard histochemistry score (H-SCORE) and the mean value was used to distinguish UBE2O high or low expression status.) and its correlation with HCG18 was analyzed by chi-square test. e Western blotting assays were used to detect the UBE2O expression after changing HCG18 in the indicated cells. f UBE2O was overexpressed in MDA-MB-231HCG18-KD cells (MDA-MB-231HCG18-KD+UBE2O) and knocked down in MCF-7HCG18 cells (MCF-7HCG18+UBE2O-KD). Then western blotting assays were performed to examine the expression changes of EMT markers (E-cadherin and vimentin), metastatic markers (MMP-2 and MMP-9) and CSPs markers (CD44, OCT4 and ABCG2) in the indicated cells. The data are shown as the mean ± s.d. Student's t test was used for statistical analysis: *$p < 0.05$, **$p < 0.01$, ***$p < 0.001$. The data represent at least three independent experiments.

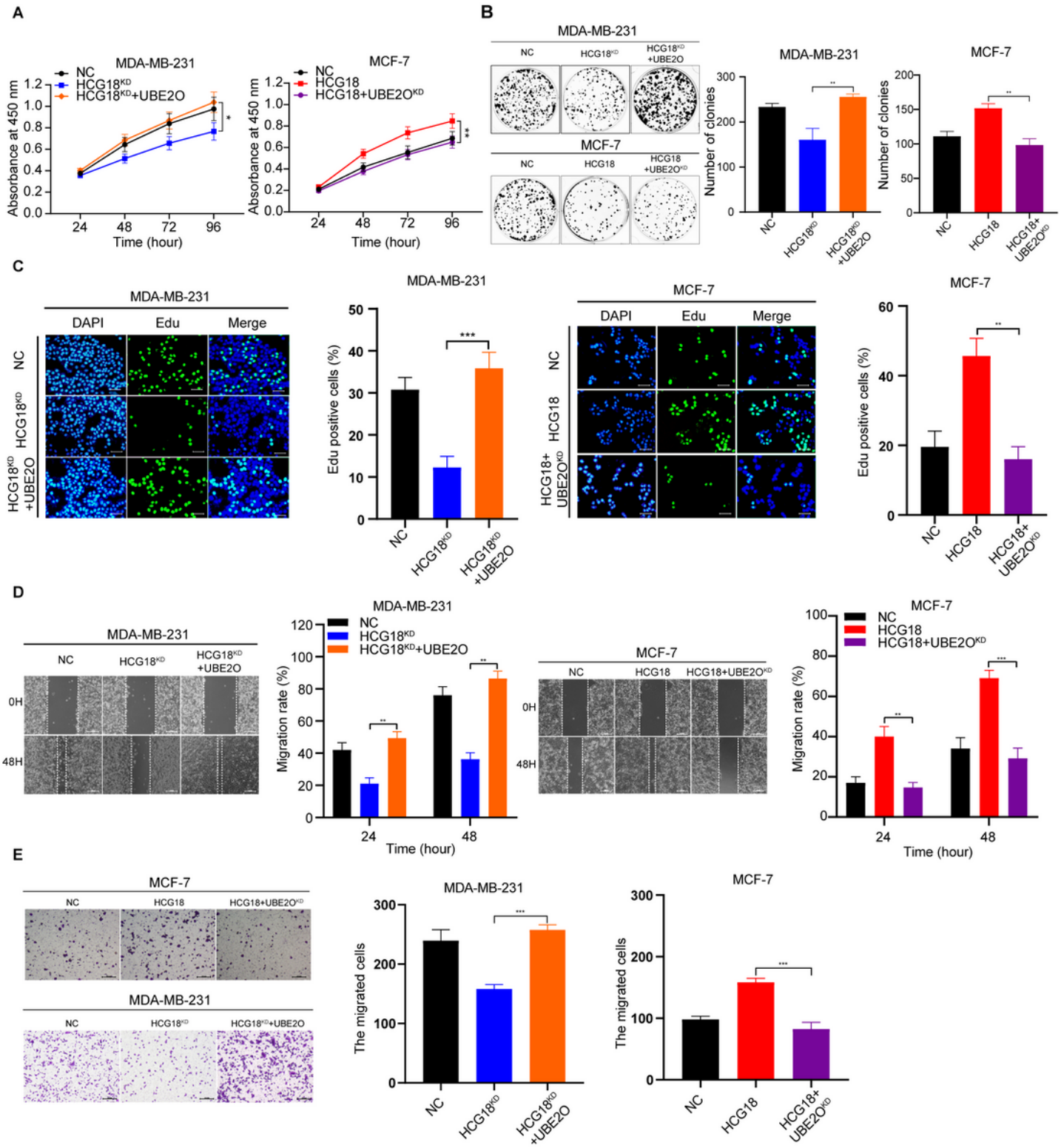

Figure 5

a-c CCK-8 (a), colony formation (b) and Edu staining assays (c) were used to measure the proliferation capabilities in MDA-MB-231NC/MDA-MB-231HCG18-KD/MDA-MB-231HCG18-KD+UBE2O and MCF-7NC/MCF-7HCG18/MCF-7HCG18+UBE2O-KD cells. d-e UBE2O was changed in MDA-MB-231 and MCF-7 cells, then scratch assays (d) and invasion assays (e) were performed. The data are shown as the mean ±

s.d. Student's t test was used for statistical analysis: *p < 0.05, **p < 0.01, ***p < 0.001. The data represent at least three independent experiments.

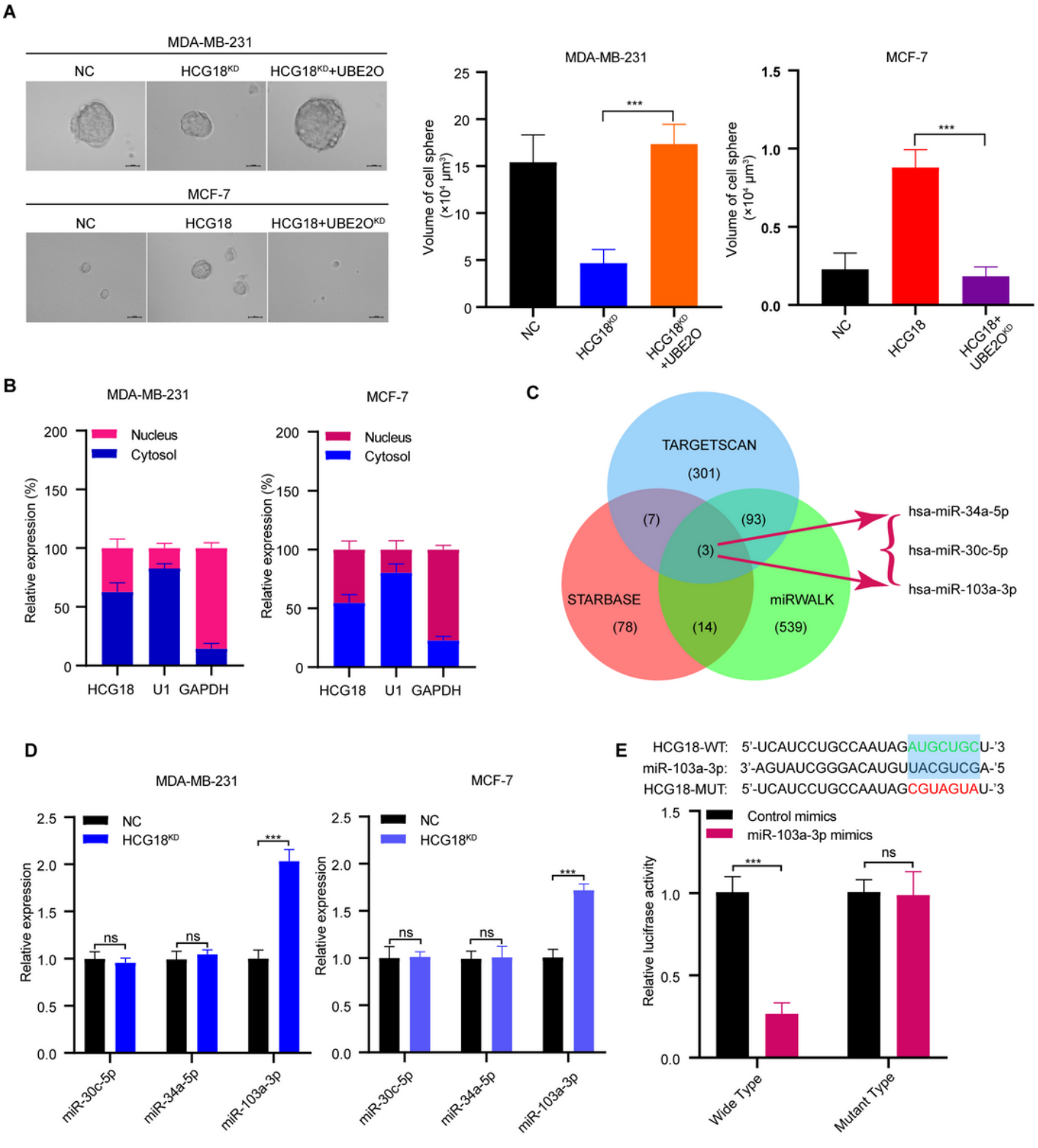

Figure 6

a Sphere formation assays were performed to detect the sphere formation capabilities in the indicated cells after changing UBE2O expression. b Nucleo-cytoplasmic separation assays were used to measure the expression levels of HCG18 in different subcellular fraction in BC cells. c Schematic illustration

showed the overlapping miRNAs targeting both HCG18 and UBE2O using Targetscan, miRWalk and Starbase database. d qRT-PCR was used to measure the expression level of predicted miRNAs in MDA-MB-231NC/MDA-MB-231HCG18-KD and MCF-7NC/MCF-7HCG18-KD cells. e HCG18-Wt/HCG18-mut and miR-103a-3p mimics were co-transfected into HEK-293T cells, then dual-luciferase reporter assays were performed. The data are shown as the mean ± s.d. Student's t test was used for statistical analysis: *p < 0.05, **p < 0.01, ***p < 0.001. The data represent at least three independent experiments.

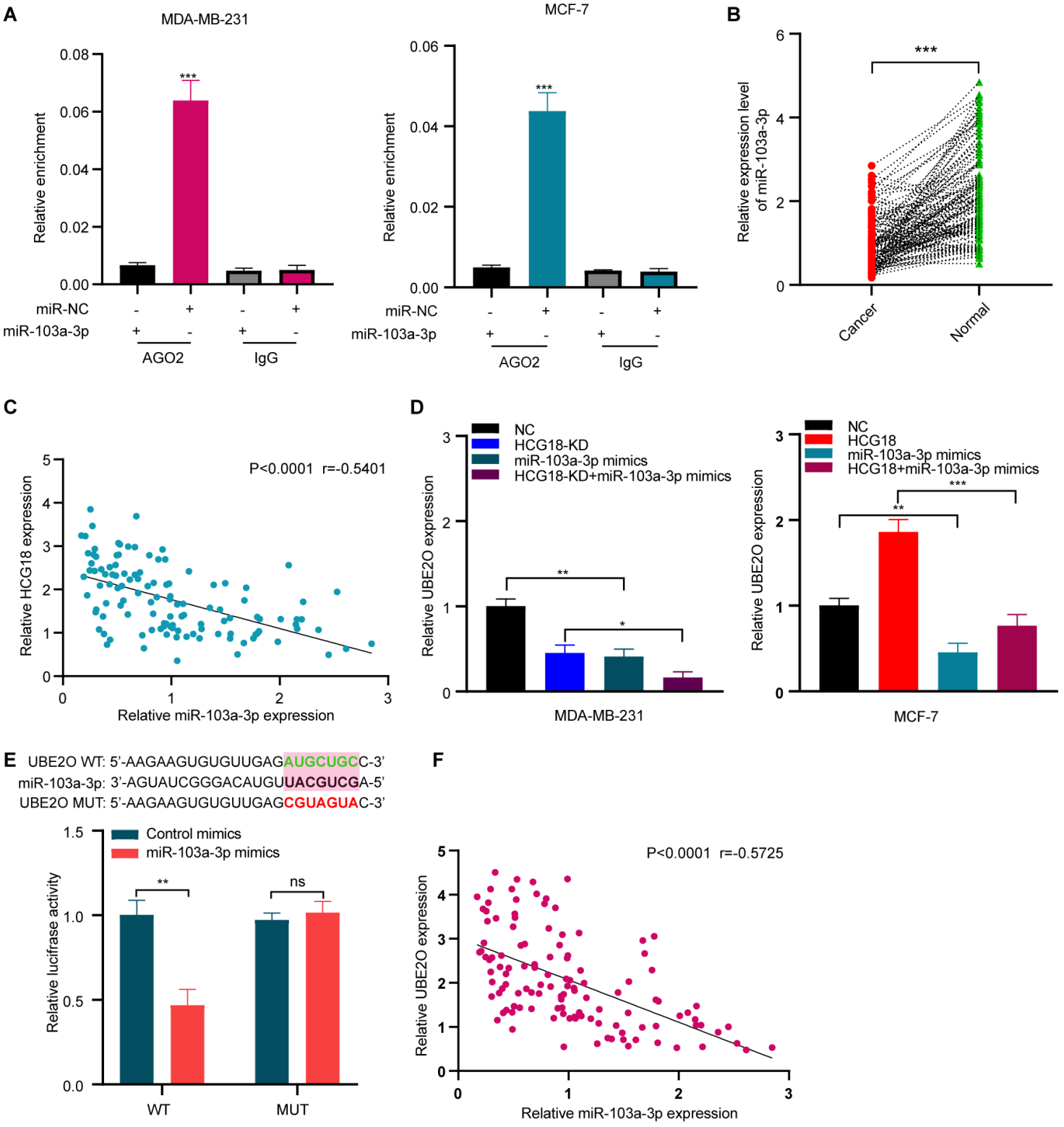

Figure 7

a Anti-AGO2 RIP assays were performed in BC cells transfected with miR-103a-3p mimics or NC, followed by qRT-PCR to detect HCG18. b-c The expression level of miR-103a-3p in BC tissues and compared normal tissues was measured by qRT-PCR (b), and its correlation with HCG18 was determined by correlation analysis (c). d miR-103a-3p mimics were transfected into MDA-MB-231NC/MDA-MB-231HCG18-KD and MCF-7NC/MCF-7HCG18 cells, then qRT-PCR was used to examine the expression changes of UBE2O in the indicated cells. e UBE2O-Wt/UBE2O-Mut and miR-103a-3p mimics were co-transfected into HEK-293T cells, then dual-luciferase reporter assays were performed. f Pearson's correlation coefficient was employed to analyze the relationship between miR-103a-3p and UBE2O in BC patients. The data are shown as the mean ± s.d. Student's t test was used for statistical analysis: *$p < 0.05$, **$p < 0.01$, ***$p < 0.001$. The data represent at least three independent experiments.

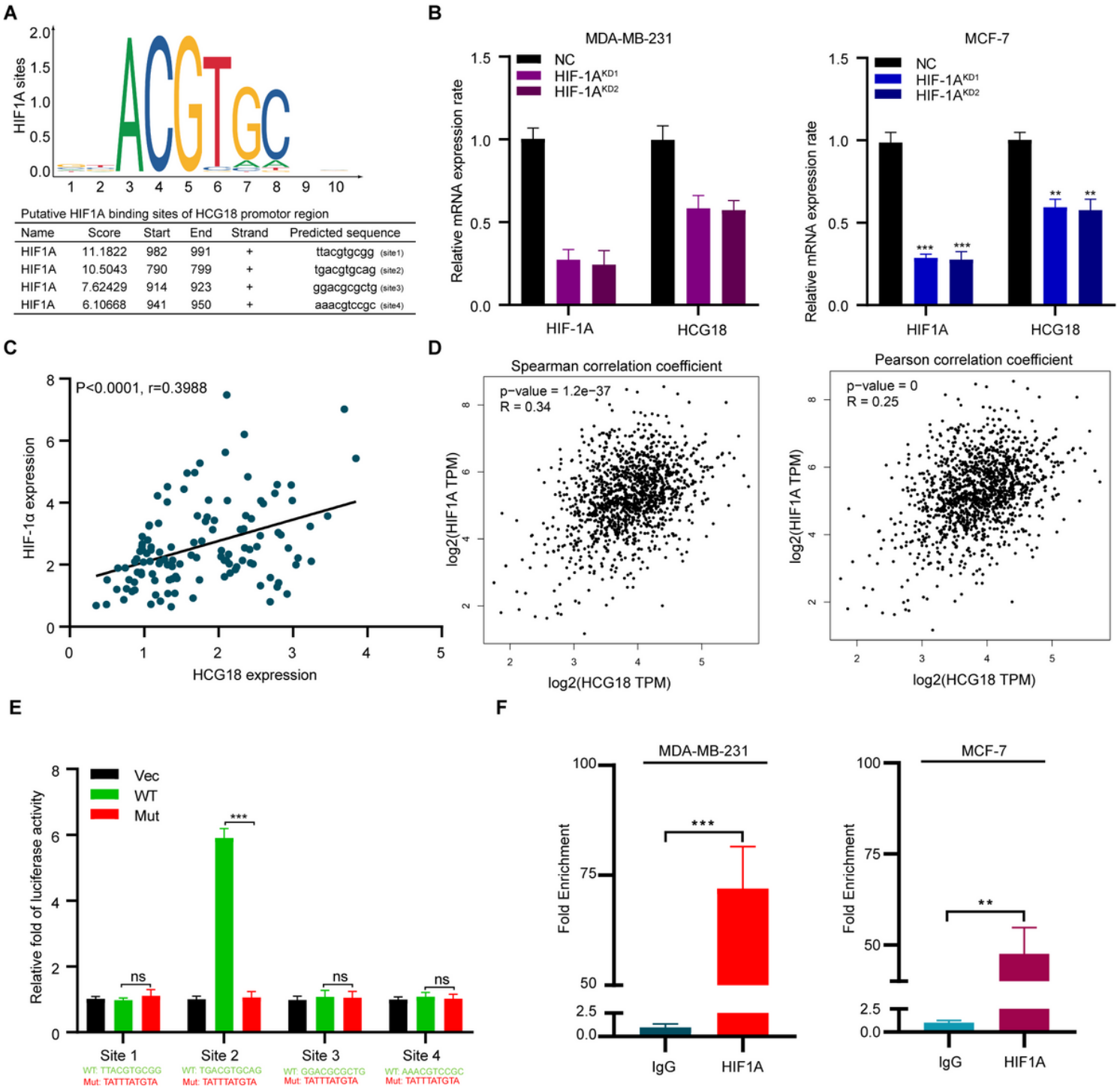

Figure 8

a HIF-1α was predicted as a potential transcription factor of HCG18 by JASPAR database, and the putative binding sites were listed. b HIF-1α was knocked down in MDA-MB-231 and MCF-7 cells, then qRT-PCR was used to measure the expression level of HIF-1α and HCG18 in the indicated cells. c HIF-1α was detected by qRT-PCR in BC tissues, and its correlation with HCG18 was analyzed by Pearson's correlation coefficient. d Results from GEPIA showed that there was a positive correlation between HIF-1α and HCG18 in BC. e Wild-type or mutant HCG18 promoter reporter constructs targeting the four binding sites of HIF-1α were separately transfected into 293 T cells, and HIF-1α plasmids were also transfected and

dual-luciferase reporter assays were performed. f ChIP assays were performed in the indicated BC cells with IgG or HIF-1α antibodies. The fragments of the HCG18 promotor region were detected by qRT-PCR. The data are shown as the mean ± s.d. Student's t test was used for statistical analysis: *p < 0.05, **p < 0.01, ***p < 0.001. The data represent at least three independent experiments.

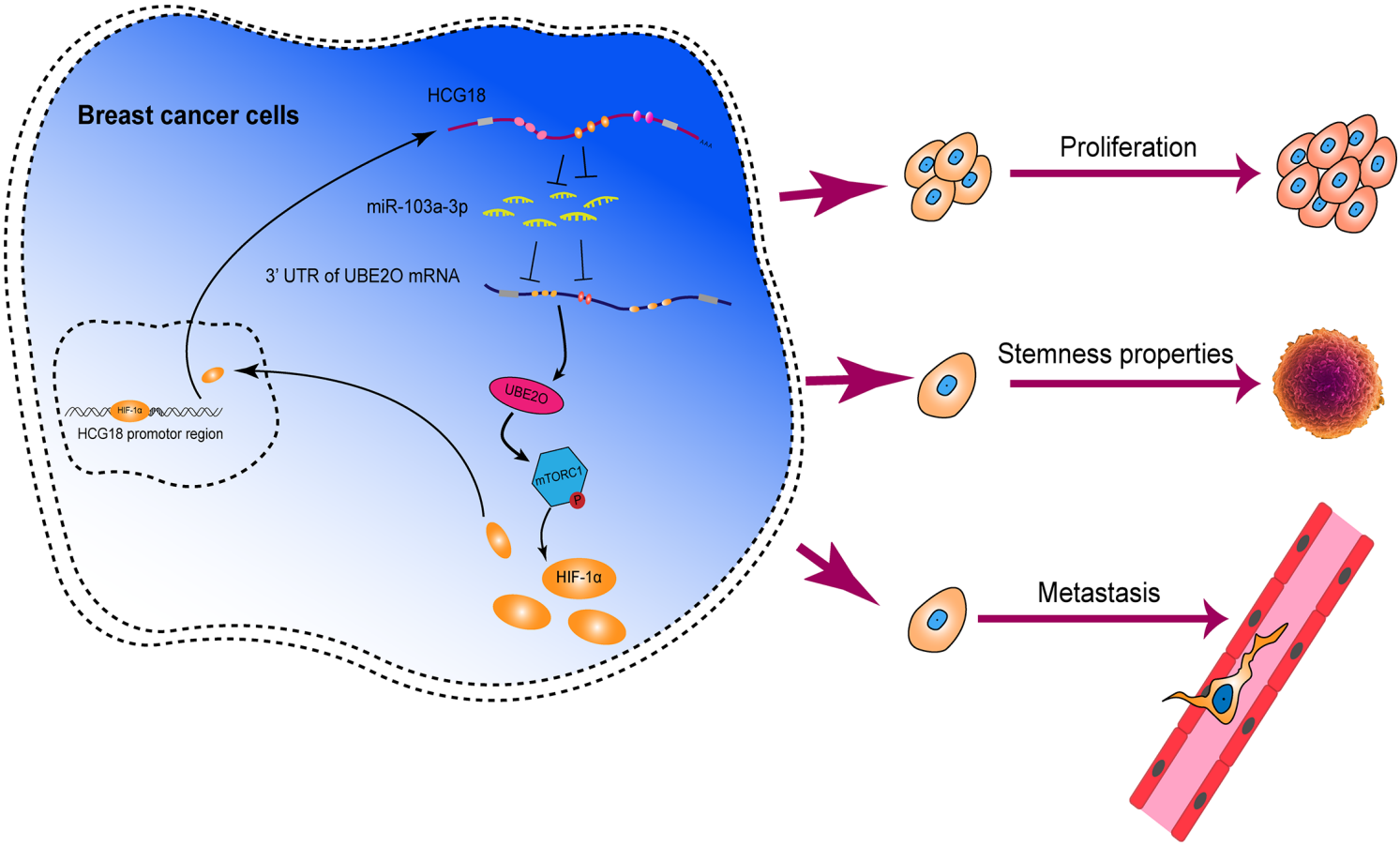

Figure 9

The schematic diagram of the oncogenic role of HCG18 in BC cells. HCG18/miR-103a-3p/UBE2O/HIF-1α axis constituted a positive feedback loop in BC cells, which played an oncogenic role in BC pathogenesis.

Supplementary Files

This is a list of supplementary files associated with this preprint. Click to download.

- supplementaryinformation.docx
- Figure.S1.tif